

## AIP Mapping of HTEM data

Simcoe Geoscience Limited is pleased to announce a new geophysical service that we are offering to extract Cole-Cole parameters from helicopter time-domain electromagnetic (HTEM) data.

In general the data acquired by the helicopter time-domain electromagnetic (HTEM) systems mainly reflect two physical phenomena of the ground: (1) Electromagnetic (EM) induction, related to the ground conductivity and governed by Faraday's Law, and (2) Airborne Induced polarization (AIP) effect related to the relaxation of polarized charges in the ground. In mineral exploration, potential near-surface sources of AIP are mainly clay sediments through membrane polarization (electrical energy stored at boundary layer), disseminated metallic sulfides and oxides (Kratzer & Macnae 2012, and Macnae 2016) through electrode polarization (electrical charges accumulated through electrochemical diffusion at ionic-electronic conduction interfaces).

Pelton et al. (1978) were the first to use the Cole-Cole impedance model (Cole & Cole, 1941) to explain the frequency dependence of resistivity observed in IP/resistivity surveys. The Cole-Cole resistivity  $\rho(\omega)$  can be expressed as,

$$\rho(\omega) = \rho_0 \left[ 1 - m \left( 1 - \frac{1}{1+(i\omega\tau)^c} \right) \right] \quad (1)$$

where  $\rho_0$  is the low frequency asymptotic resistivity in  $\Omega \cdot m$ ,  $m$  ( $0 \leq m \leq 1.0$ ) is the dimensionless chargeability,  $\tau$  is the relaxation time-constant in seconds and  $\omega = 2\pi f$  the angular frequency, and finally  $c$  ( $0 \leq c \leq 1.0$ ) is the frequency factor. The four Cole-Cole parameters ( $\rho_0$ ,  $m$ ,  $\tau$  and  $c$ ) are characteristic of the intrinsic polarizability of the ground. In general, the chargeability  $m$  and relaxation time-constant  $\tau$  depend on the quantity and size of polarizable material respectively (Pelton et al., 1978). The frequency factor reflects the size distribution of the polarizable elements (Luo and Zhang, 1998). *Sensu stricto* the parameter  $\rho_0$  is related to EM induction and only the parameters ( $m$ ,  $\tau$  and  $c$ ) are associated with the AIP effect.

AIP mapping is the extraction of the four Cole-Cole parameters ( $\rho_0$ ,  $m$ ,  $\tau$  and  $c$ ) from a single HTEM decay without deriving the depth distribution of the parameters. The extraction of Cole-Cole parameters from field HTEM data has been carried out by Kratzer and Macnae (2012), Hodges and Chen (2014), Kwan et al. (2015), Macnae (2016), Kang et al. (2017), Kaminski and

Viezzoli (2017) and, more recently, Kwan and Müller (2020). A new AIP mapping method capable of extracting all four Cole-Cole parameters from HTEM data has been developed and presented by Kwan and El-Kaliouby (2020).

The new AIP mapping method is applied to HTEM (VTEM, Witherly et al., 2004) data from Tli Kwi Cho (TKC) kimberlite complex, NWT, Canada. The TKC consists of two pipes, namely DO18 (north) and DO27 (south). The survey was flown at nominal line spacing of 75 m, and the data were made available to the public through the University of British Columbia Geophysical Inversion Facility in 2016. The AIP signatures of the two kimberlites were thoroughly investigated by Kang et al. 2017.

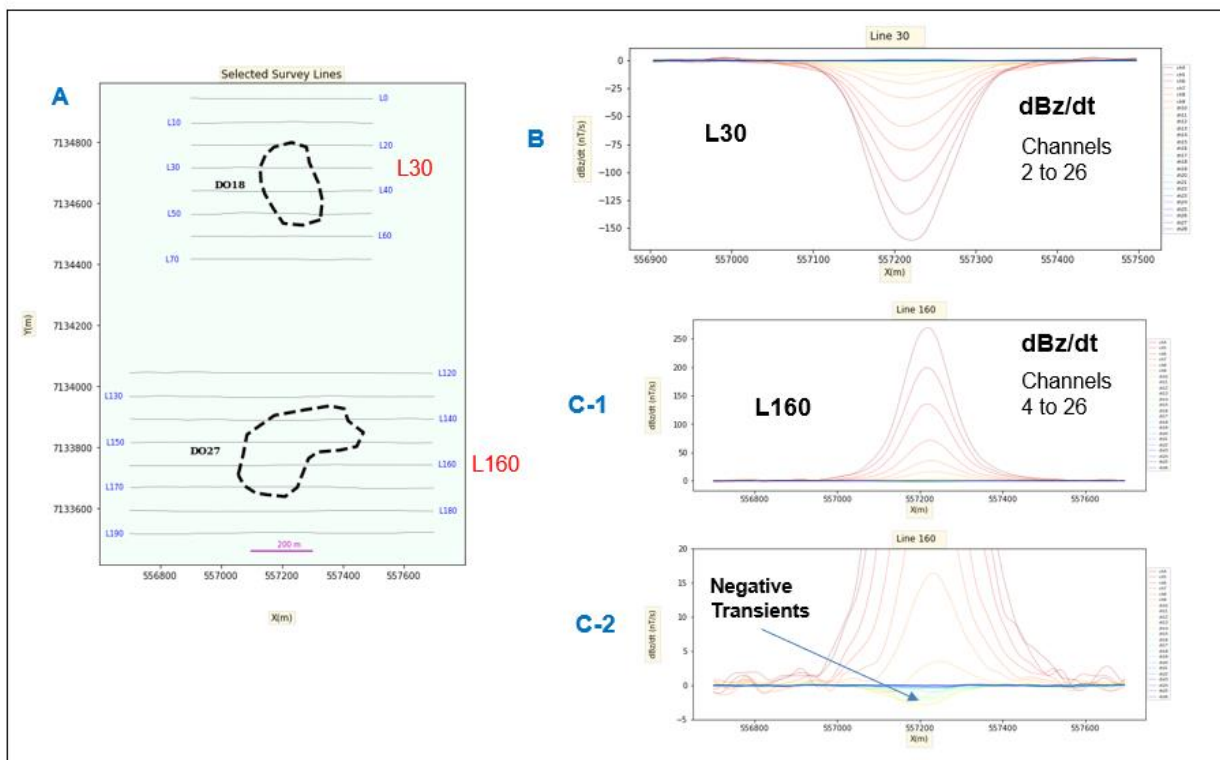


Figure 1: dBz/dt profiles of L30 over DO18 (north) and L160 over DO27 (south).

The derived AIP apparent resistivity and apparent chargeability data are shown in Figure 2. The ground over DO27 are more conductive ( $\sim 300 \Omega \cdot m$ ) than that over DO18 ( $\sim 1200 \Omega \cdot m$ ). The apparent resistivity results over DO27 and DO18 compare reasonably well with those derived by

Kang et al. (2017). The ground over DO27 is relatively more chargeable than DO18. Results derived by Kang et al. (2017) showed that DO27 is more chargeable than DO18 as well.

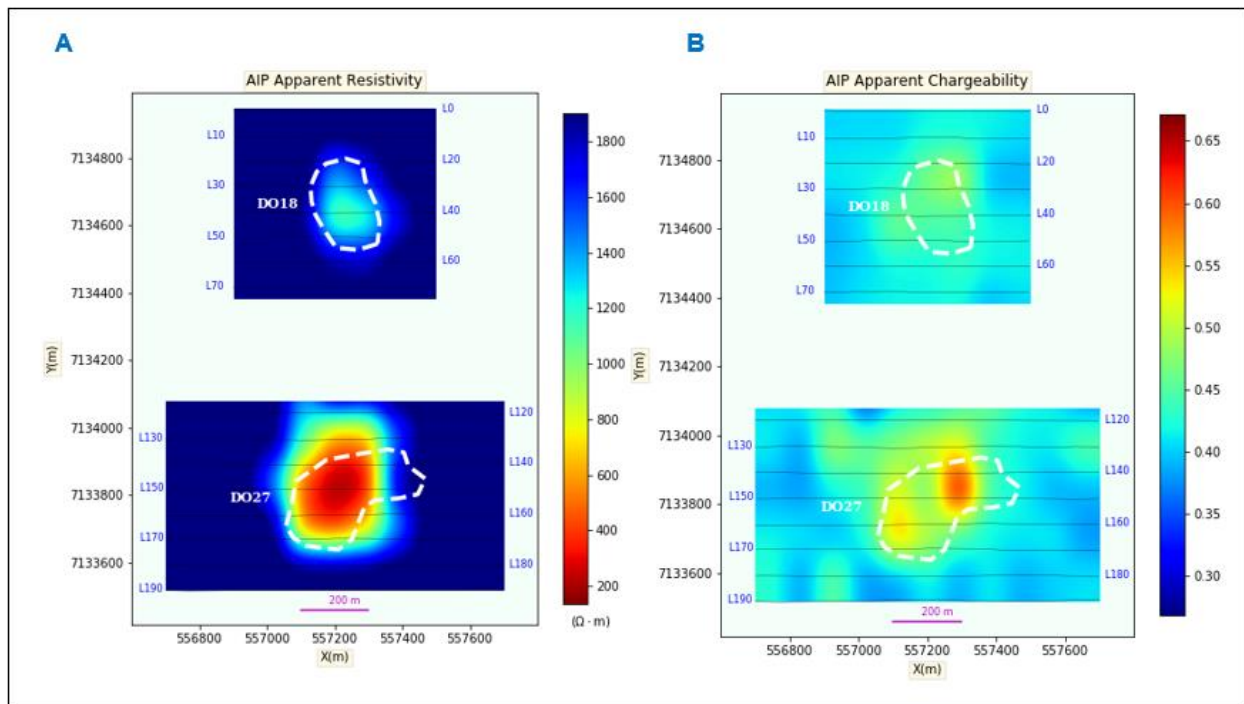


Figure 2: (A) AIP apparent resistivity and (B) apparent chargeability data.

Displayed in Figure 3 are the AIP relaxation time-constant and frequency factor data. The relaxation time-constants are low over DO18 and are relatively high over DO27. The frequency factors over DO18 are higher ( $\sim 0.8$ ) than those over DO27 ( $\sim 0.6$ ). The relaxation time-constants and frequency factors of DO18 suggest that the polarizable materials are more uniformly distributed and fine-grained. On the other hand, the sizes of the grains of the polarizable material in DO27 are relatively larger than those in DO18. Kang et al. (2017) suggest that the polarizable source may be a frozen ice/clay mixture at DO-18 and conductive clay for DO-27.

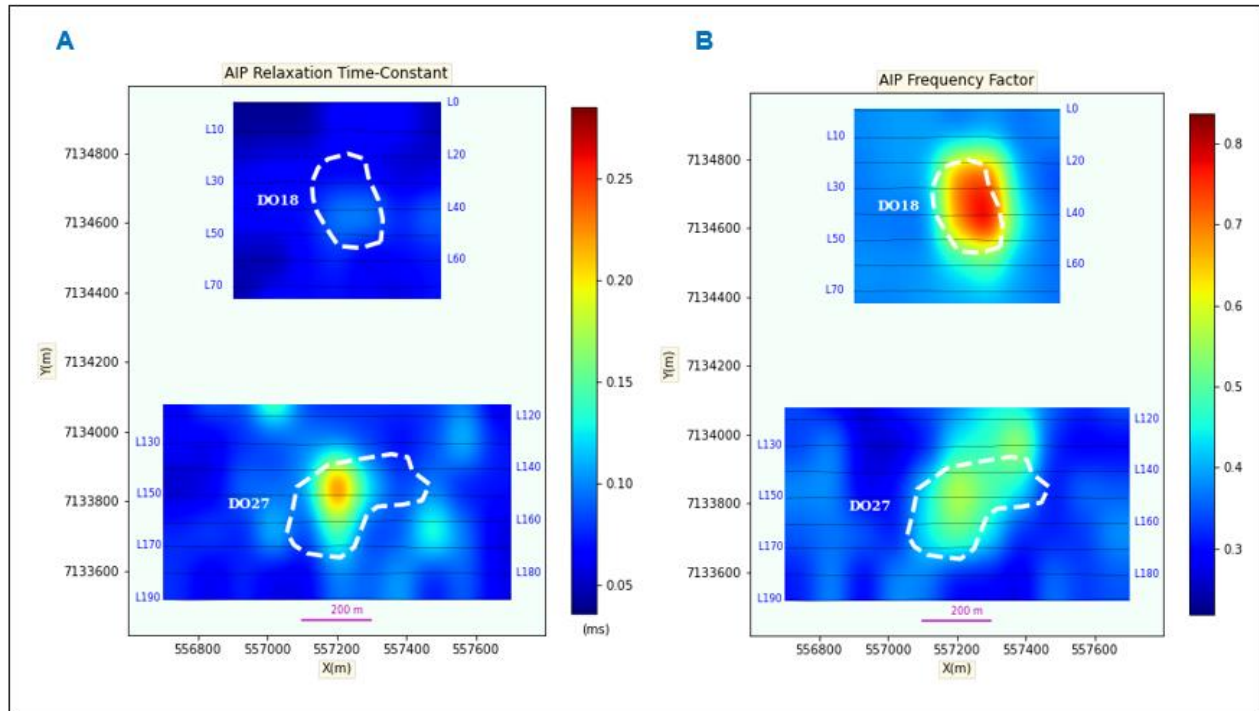


Figure 3: (A) AIP relaxation time-constant and (B) frequency factor data.

The new AIP mapping method can extract subtle IP signatures from HTEM data. The extracted IP responses could be used as vectoring tools for the search for potential hydrothermally related mineralization and economic deposits, such as alkalic porphyry Au-Cu systems (Kwan & Müller, 2020) and Archean lode gold (Müller, Kwan & Groves, 2020, submitted).

## References

Hodges, G., and Chen, T.Y., 2014. IP effect in airborne TDEM data: model studies and field examples, expanded abstract, SEG Denver 2014 Annual Meeting.

Kaminski, V. and Viezzoli, A., 2017. Modeling induced polarization effects in helicopter time-domain electromagnetic data: Field case studies, **82** (2), B49-B61.

Kang, S., Fournier D. and Oldenburg D., 2017. Inversion of airborne geophysics over the DO-27/DO-18 kimberlites – part 3: induced polarization. *Interpretation* 5: T345–358.

Kratzer, T. and Macnae, J.C., 2012. Induced polarization in airborne EM. *Geophysics* 77: E317-327.

Kwan, K., Prikhodko, A., Legault, J.M., Plastow, G., Xie, J. and Fisk, K., 2015. Airborne Inductive Induced Polarization Chargeability Mapping of VTEM data; ASEG-PESA 24th International Geophysical Conference and Exhibition, Perth, Australia.

Kwan, K. and Müller, D., 2020. Mount Milligan alkalic porphyry Cu-Au deposit, British Columbia, Canada, and its AEM and AIP signatures: Implication for mineral exploration in covered terrains, *Journal of Applied Geophysics*, 104131; <https://doi.org/10.1016/j.jappgeo.2020.104131>.

Kwan, K., El-Kaliouby, H., 2020. Airborne Induced Polarization (AIP) mapping of HTEM data: method and tests. *Journal of Applied Geophysics* (submitted).

Luo, Y. and Zhang, G., 1998. Theory and application of Spectral Induced Polarization; *Geophysical Monograph Series*.

Macnae, J., 2016. Quantifying airborne induced polarization effects in helicopter time domain electromagnetics: *Journal of Applied Geophysics*, **135**, 495-502.

Müller, D., Kwan, K., and Groves, D.I., 2020: Structural and geophysical implications for the exploration of concealed orogenic gold deposits: a case study in the Sandy Lake and Favourable Lake Archean greenstone belts, Superior Province, Ontario, Canada. *Ore Geology Reviews* (submitted).